Springer

KSME

Journal of Mechanical Science and Technology 25 (5) (2011) 1167~1174
www.springerlink.com/content/1738-494x
DOI 10.1007/s12206-011-0306-2

Evaluation of surface cracking in micron and sub-micron scale scratch tests for optical glass BK7 †

Weibin Gu[1,*] and Zhenqiang Yao[1,2]

[1]*School of Mechanical and Power Engineering, Shanghai Jiao Tong University, Shanghai, 200240, China*
[2]*State Key Laboratory of Mechanical System and Vibration, Shanghai Jiao Tong University, Shanghai, 200240, China*

(Manuscript Received June 29, 2010; Revised December 19, 2010; Accepted February 16, 2011)

Abstract

In order to obtain the fundamental information on the deformation and fracture behavior of brittle materials during precision and ultra-precision grinding, micron and sub-micron scale scratch tests were conducted on optical glass BK7 using Vickers indenters. Three types of surface cracking were observed around the scratch grooves. They are lateral cracking, radial cracking and cracking in front of the moving indenter. It is found that lateral cracking is the main damage type due to its large damage size and low crack initiation load. The effect of surface cracking on the relationship between the normal load and the square of scratch depth was studied. The plastic zone size as well as the sliding blister field strength was expressed as a function of the contact zone size of the indenter. A prediction model for the size of damage zone induced by lateral cracking was established and was compared with experimental results.

Keywords: Micron and sub-micron scale; Optical glass BK7; Scratch test; Surface cracking

1. Introduction

BK7 glass is widely used for high quality optical components because it is almost bubble-free and has low amount of inclusions. Grinding process is one of the most important finishing operations for high precision glass components. However, due to its hard and brittle nature, BK7 is generally considered to be difficult to grind. It is known that the interaction between the hard particles and the brittle material may induce various cracks and therefore influence material removal mechanism and surface quality. To obtain the fundamental information on the deformation and fracture behavior of brittle materials, scratch processes were studied by many researchers [1-12].

Lateral cracking is considered to be one of the main cracking types induced by scratching [6-9]. V.L. Houérou et al. [8] systematically investigated surface damage of soda-lime-silica glasses during single scratch processes. They found that lateral crack propagation toward the scratched surface led to large chipping and thus to material removal. Klecka and Subhash [9] conducted double scratch tests for alumina ceramics to study the fundamental behavior of interacting pairs of scratches. It was found that the interaction between lateral cracks generated around neighboring scratch grooves was the principal mechanism for material removal.

Some studies were focused on modeling the fracture characteristics of brittle materials using analytical approaches [10-13]. Yoffe [10] utilized a doublet force system to enforce a traction-free boundary condition outside the contact impression on the top surface. The strength of blister field A was established to calculate the residual elastic-stress field due to plastic deformation in indentation process. In order to estimate the residual stress field in scratch process, Ahn et al. [11] introduced the strength of sliding blister field B which is a function of the strength of the blister field A and the increment of the scratch depth. The residual stresses near the lateral crack and the stress intensity factor at the crack tip were elastic-mechanically modeled by Ahn et al. [12]. They also developed a theoretical model for predicting the length of lateral crack. However, due to the simple assumption about the occurring point of the lateral crack and the shape of the plastic zone, the predicted length was about half of the experimentally measured length. Jing et al. [13] also proposed a model for investigating deformation and induced damage associated with a single scratch in brittle materials. Based on the Rankine criterion for brittle fracture, the damage zone size induced by lateral cracking was quantitatively estimated during a scratch process. Although the prediction model was found to be agreement with the available FE simulation results in literature, the comparison between the prediction model and the experi-

† This paper was recommended for publication in revised form by Associate Editor Chongdu Cho

* Corresponding author. Tel.: +86 21 34206583, Fax.: +86 21 34206315
E-mail address: alexgwb@gmail.com

mental results was not available.

In this study, micron and sub-micron scale scratch tests were made on optical glass BK7 using Vickers indenters. The surface cracking induced by scratching, the relationship between the normal load and the s quare of the scratch depth and the typical profile of scratch groove were analyzed. A prediction model for the size of damage zone induced by lateral cracking was proposed and was compared with experimental results as well as Jing's model mentioned above.

2. Experimental procedure and results

The size of optical glass BK7 used in scratch test was 20mm×10mm×5mm. To minimize damage incurred during previous machining, the square surfaces were polished with cerium dioxide powder of 1-3μm grit size and observed under an optical microscope.

Scratch tests were performed using Lateral Force Measurement (LFM) technique attached to a Nano Indenter XP. For each test, an initial specimen surface profile before scratching was obtained by pre-scanning the sample surface with the indenter under a very low load of 20μN. During scratching, the scratch depth and the applied load were recorded. After scratching, the surface profile of the sample was again scanned by post-scanning under conditions identical to those used in the pre-scanning.

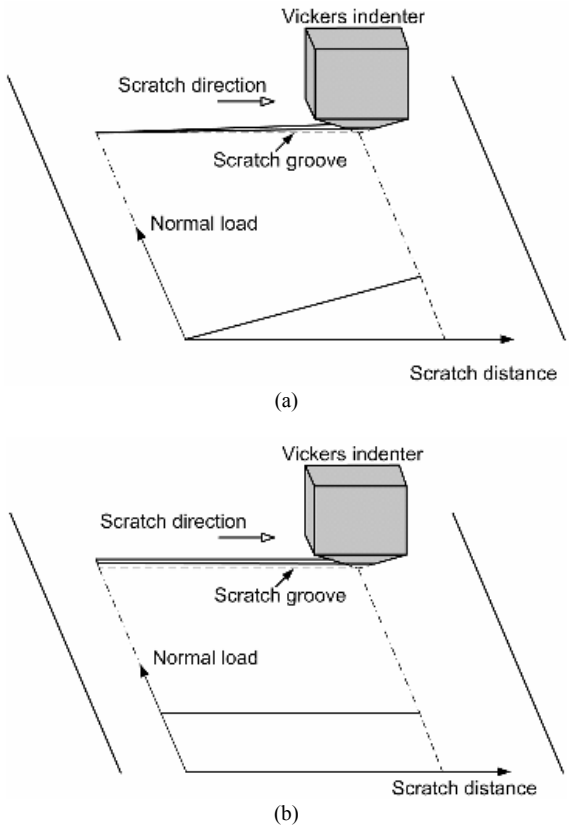

Fig. 1. Illustration of scratch tests (a) linearly increasing normal load; (b) constant normal load.

In this study, Vickers indenters, oriented in a face-leading configuration, were used for all tests. Two different loading conditions (linearly increasing normal load and constant normal load) were studied (see Fig. 1) and the respective parameters were described in Table 1. The samples and the Vickers indenter were cleaned with ethanol both before and after each test.

2.1 Microscopy observation of surface cracking

To investigate how applied normal load affect scratch cracking, both linearly increasing normal load and constant normal load scratch tests were performed and were observed by optical microscopy (see Fig. 2). At low normal loads, typically between 0~30mN, the scratch mode is predominantly ductile and the groove appears to be fully plastic due to the high local hydrostatic compressive stresses close to the tip of the indenter [14] (see Fig. 2(b)). When normal load is higher than 30mN, lateral cracking paralleling to the surface was observed on both sides of the groove (see Fig. 2(c)). These cracks are thought to nucleate near the plastic deformation zone below the contact due to residual tensile stress during unloading phase [15]. With further increase in normal load, the interaction between the front of the indenter and the specimen becomes more intense, and cracks occur in front of the moving indenter during scratch process. Then some of the cracks in front of the moving indenter probably deviate to either side of the scratch tack and lead to radial cracks along the scratch groove [15]. Moreover, the frictional forces behind the indenter may cause further propagation of radial cracks

Table 1. Summary of parameters used in scratch tests.

Young's modulus E (GPa)	82[18]
Poisson's ratio v	0.203[18]
Yield Strenss σ_y (GPa)	3.5[18]
Fracture strength σ_f (GPa)	0.048[19]
Vickers hardness H (GPa)	7.7[20]

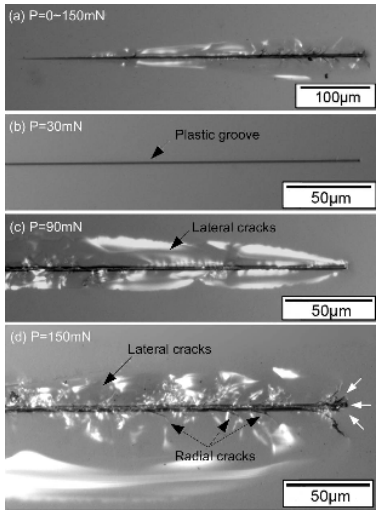

Fig. 2. Optical micrographs of scratch tests.

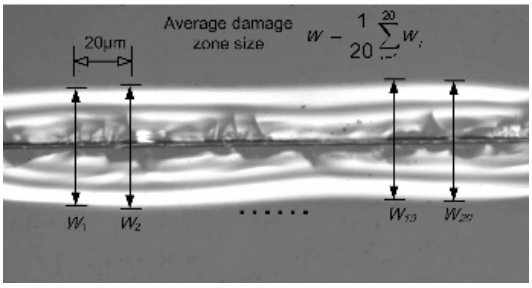

Fig. 3. Schematic of the measurement of the damage zone size.

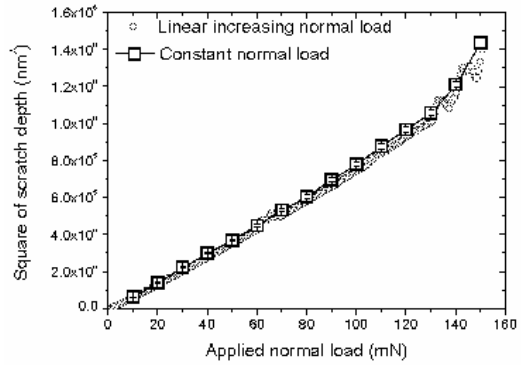

Fig. 4. The square of scratch depth vs. normal load.

[16]. As a result, both radial cracks and cracks at the end of the scratch groove (as indicated by white arrows) were observed in Fig. 2(d).

It should be noted that due to the low level of normal loads (i.e., 0~150mN), lateral cracking never reached the surface and therefore no obvious chipping was observed around the scratch groove. But in case of multi-points scratching and grinding, lateral cracks generating around neighboring scratches may intersect with each other and therefore induce chipping. Therefore, in order to obtain the fundamental information on material removal and surface quality during grinding, it is helpful to investigate how applied normal load affect the size of damage zone induced by lateral cracking experimentally and analytically. In this study, the damage zone size under a given normal load was measured twenty times along the groove with equal space distance of 20μm as illustrated in Fig. 3. In order to compare with the analytical model discussed later, the average of twenty readings under the same normal load was taken as experimental data.

2.2 Relationship between normal load and square of scratch depth

The typical relationships between the normal load and the square of the scratch depth under the two different loading conditions were shown in Fig. 4. For linear increasing normal load case, the scratch depth was recorded continuously as a function of the normal load. While for constant normal load case, the measured scratch depths at a given normal load were averaged over the scratch length and were plotted with error bars.

Table 2. Material properties of optical glass BK7.

Young's modulus E (GPa)	82[18]
Poisson's ratio v	0.203[18]
Yield Strenss σ_y (GPa)	3.5[18]
Fracture strength σ_f (GPa)	0.048[19]
Vickers hardness H (GPa)	7.7[20]

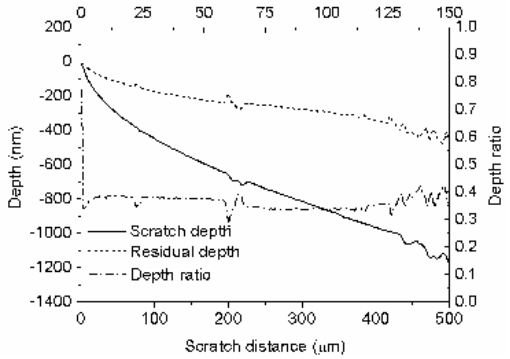

Fig. 5. Scratch depth, residual depth and depth ratio vs. normal load.

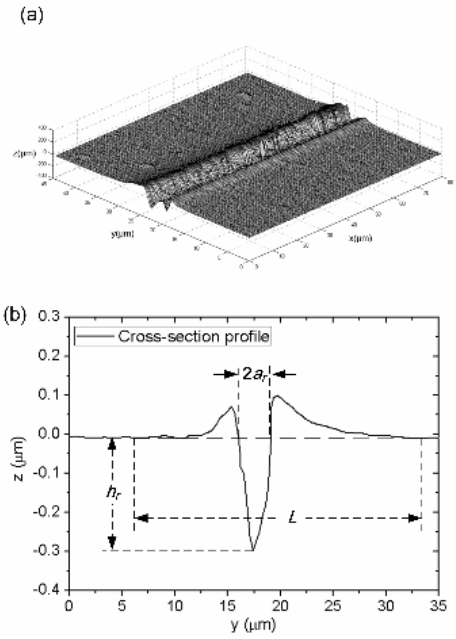

Fig. 6. The typical morphology under normal load of 90mN (a) 3D profile; (b) Cross-section profile.

It is found that the data under the two different loading conditions show a similar trend, indicating that the relationship between the applied normal load and the square of the scratch depth is insensitive to the discussed loading conditions. When normal load is less than 130mN, the square of the scratch depth increases approximately linearly with the normal load even when lateral cracks appear around the scratch groove. The main reason is that the scratch depth is measured during loading phase while lateral cracking is generated after the indenter moved away from the original location. Therefore, lateral cracking has little effect on the relationship between the

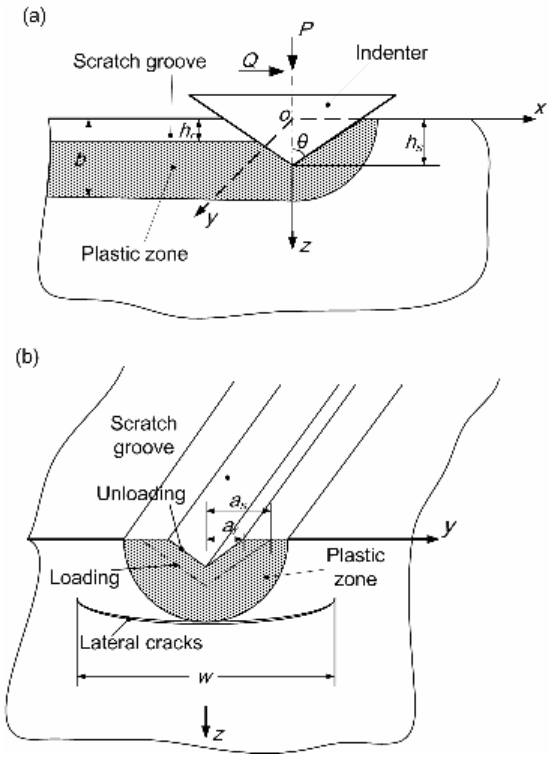

Fig. 7. Schematic of scratch groove by a sharp indenter on BK7.

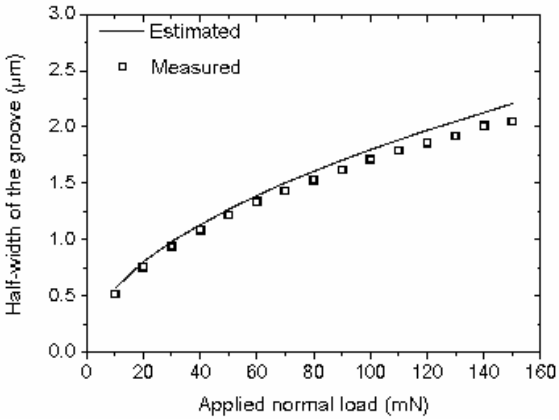

Fig. 8. The estimated and measured values of the half-width of the groove.

normal load and the square of the scratch depth. With further increase in normal load, cracking appears to occur in front of the moving indenter. As the indenter continues to move on, the strength of the material interacting with the indenter might be degraded due to the existence of the cracking. As a result, the square of the scratch depth significantly increases with the normal load in an unstable manner as shown in Fig. 4. For constant normal load scratch tests, the variability of the scratch depth also becomes more significant, which is indicated by the larger magnitude of the error bars.

2.3 Depth ratio and the profile of scratch groove

Scratch depth is the depth recorded during scratching while residual depth is the depth measured after removing the indenter. The scratch depth, the residual depth and the depth ratio defined as the ratio of the residual depth to the scratch depth were plotted as a function of the applied normal load in Fig. 5. It is seen that the residual depth is much smaller than the scratch depth, indicating the significant recovery of BK7 after complete removal of the indenter. Note that when normal load is less than 130mN, the depth ratio is almost constant. When normal load is greater than 130mN, cracks start to occur in front of the moving indenter, and the variations of the scratch depth as well as the residual depth become significant, resulting in the instability of the depth ratio.

The typical morphology under normal load of 90mN is shown in Fig. 6, and there is pileup formation on the two sides. It is interesting to compare this observation with the simulation results of the scratch tests on elastic and perfectly plastic materials made by Bucaille et al. [17]. They introduced the rheological factor: $X=E\cdot\cot\theta/\sigma_y$ (where θ is the semi-apical angle of the indenter) to evaluate the elastic-plastic behavior of scratched materials. Using material properties of BK7 from Table 2, the rheological factor is about 8.5 at which no significant pileup is expected to occur around the scratch groove. However, the pileup phenomenon of optical glass BK7 due to scratch process was observed in Fig. 6. Furthermore, it was found that the pileup zone size as shown in Fig. 6(b) is comparable to the size of damage zone induced by lateral cracking (i.e.,$L\approx W$). This result indicates that the 'pileup' phenomenon might be associated with the lift up of scratched surface due to the existence of lateral cracking.

3. Theoretical analysis of lateral cracking

3.1 Residual stress fields in the elastic zone beneath the contact

As shown in Fig. 7, when both the normal load P and the tangential load Q are applied on the moving indenter, the indenter penetrates into the specimen with the scratch depth h_s and the half-with of the contact area a_s. A plastic deformation zone with the depth b is generated beneath the indenter. After the completely removal of the indenter, the scratch groove is left on the specimen with the residual depth h_r and the half-width a_r of the scratch groove. In situ observations indicate that lateral cracking initiates near the plastic deformation zone below the contact and the subsequent growth occurs in the elastic region [11]. Therefore, only elastic deformation is of interest in this study. The stress distribution in the elastic region caused by the sliding indentation could be obtained as the superposition of three stress fields – the Boussinesq field, the Cerruti field and the sliding blister field. The first two stress fields were given by Johnson [21] and the last one was derived by Ahn et al. [11].

Moreover, lateral cracking was observed to initiate and propagate due to the residual tensile stress during unloading phase [15]. The residual stress components could be obtained by assuming a 2-D plane strain condition and calculating the stress far behind the moving indenter [13]:

$$\sigma_{yy} = 2B\left(\frac{6y^2\left(-y^2+2z^2\right)}{\left(y^2+z^2\right)^3}\right) \tag{1a}$$

$$\sigma_{zz} = 2B\left(\frac{4z^2\left(-3y^2+4z^2\right)}{\left(y^2+z^2\right)^3}\right) \tag{1b}$$

$$\tau_{yz} = 2B\left(\frac{-8yz\left(y^2-z^2\right)}{\left(y^2+z^2\right)^3}\right) \tag{1c}$$

where B is the strength of the sliding blister field mentioned above. The origin of the coordinate system o could be determined by projecting the tip of the moving indenter to the specimen surface along the vertical direction (see Fig. 7). The positive x-direction is the scratch direction, the positive z-direction is towards the indentation depth of the scratched material, and the positive y-direction is perpendicular to the xz plane.

3.2 Estimation of half-width of the groove a_r and plastic zone size b

The hardness is typically defined as the applied load divided by the impression size. Due to the analogy between indentation hardness and scratch hardness, the half-width of the groove a_r, induced by a Vickers indenter with a face-leading configuration, could be expressed as

$$a_r = \frac{1}{2}\sqrt{\frac{P}{H}} \tag{2}$$

where P is the normal load and H the Vickers hardness. The half-width of the scratch groove h_r was also measured from the cross-section profile as shown in Fig. 6. Comparison of the experimental results with the values from Eq. (2) in Fig. 8 reveals that there is a good agreement between the measured and estimated values.

Experimental observations indicate that lateral cracking initiate at or close to the boundary between the inelastic deformation zone and the surrounding elastic solids and spread out laterally on a plane closely parallel to the specimen surface [15]. Therefore, the depth of lateral cracks could be approximated as the plastic zone depth b. The relationship between the plastic zone size b and the contact size a_s was derived by Jing et al. [13]:

$$b = a_s\left[\frac{3(1-2v)}{5-4v} + \frac{2\sqrt{3}}{\pi(5-4v)}\frac{E}{\sigma_y}\cot\theta\right]^{1/2}. \tag{3}$$

As we know, it is not easy to measure the contact size of the indenter during scratch process. Therefore, it is commonly assumed that the contact size of the indenter is the same as the half-width of the scratch groove (i.e.,a_s=a_r) [13]. This assumption is suitable for metals which are very plastic, but might not be reasonable if the recovery of the scratched material is non-neglectable. As mentioned in Section 2.3, the residual depth is much smaller than the scratch depth, indicating the significant recovery of optical glass BK7. Therefore, the half-width of the scratch groove is also expected to be smaller than the contact size of the indenter. Furthermore, Ramond-Angélélis [22] found that during indentation, the ratio of the residual width to the width under load is close to the ratio of the residual depth to the depth under load. Based on the analogy between indentation and scratch process (that is, scratch testing could be regarded as a series of indentations along the scratch direction), we assumed that the ratio of the half-width of the groove to the contact size was equal to the residual depth to the scratch depth:

$$a_r/a_s = h_r/h_s = \mu \tag{4}$$

where μ is the depth ratio demonstrated in Section 3.3. By substituting Eq. (4) into Eq. (2), the contact size could be calculated:

$$a_s = \frac{1}{\mu}\cdot a_r = \frac{1}{2\mu}\cdot\sqrt{\frac{P}{H}}. \tag{5}$$

3.3 Estimation of strength of the sliding blister field

To develop an explicit expression of the sliding blister field strength B, we use the relationship between the increased volume in inelastic deformation zone during an indentation ΔV_i and that during a scratch ΔV_s. Yoffe [10] derived the expression of ΔV_i:

$$\Delta V_i = 2\pi A\frac{1-2v}{3G} \tag{6}$$

where G is the shear modulus, v is the Poisson's ratio and A is the strength of indentation-induced blister field. Ahn et al. [11] treated the accumulated blister field due to sliding by taking the strength of the blister filed per unit sliding length, B, as $A=B(\xi)d\xi$, where $d\xi$ is the increment of the scratch length.

During indentation the volume displaced through any hemisphere centered on the center of expansion is constant and is equal to the volume of the contact impression [23]. Based on the similarity of the indentation and scratch processes, we approximated the increased volume in inelastic deformation zone during a scratch as the impression volume of the sliding indentation after complete removal of the indenter. Based on the analysis of the "pileup" effect of BK7 in Section 3.3, we assumed that the pileup due to elastic-plastic deformation is negligible. This is consistent with the assumption for the scratch groove of brittle solids made by Jing et al. [13]. As a result, the increased volume in inelastic deformation zone during a scratch could be expressed:

$$\Delta V_s = \frac{a_r^2}{\tan\theta}\cdot l \tag{7}$$

where a_r is the half-width of the scratch groove and l is the scratch length.

Using the relationship $A=Bd\zeta$ in Eq. (6) and integrating over the scratching line from l to 0, and equating to Eq. (7), we obtained:

$$B=\frac{3a_r^2E}{4\pi(1-2\nu)(1+\nu)}\cot\theta. \tag{8}$$

By substituting Eq. (5) into Eq. (8), we obtained the expression of the sliding blister field strength:

$$B=k\frac{3a_s^2E}{4\pi(1-2\nu)(1+\nu)}\cot\theta \tag{9}$$

where $k=\mu^2$. Jing et al. [13] have also developed the similar explicit expression for the sliding blister field strength with $k=f$. It should be noted that the parameter k in the present model was based on the measurement of the residual and scratch depths while the determination of the parameter k by Jing et al. was from the relationship $f \bullet E/H=1.09$ for sharp indentation [23]. For optical glass BK7, the parameter f is about 0.11, which is in reasonable agreement with the value of μ^2 (≈0.102). It is noted that when the scratched material and the indenter are determined, the half-width of the contact area a_s is dependent on the applied normal load. As a result, the parameter B depends on the material properties of the specimen and the geometry of the indenter as well as the scratch parameters.

3.4 Prediction of the size of damage zone induced by lateral cracking

To estimate the damage zone size due to lateral cracking, we assumed that: (i) lateral cracks initiate in mode I according to the Rankine failure criterion; (ii) the local stress concentration at the crack tip is not taken into account; (iii) crack initiation sites encompass the entire damage zone. Based on the above assumptions, we could suppose that lateral cracks will propagate on the plane $z=b$ until the maximum tensile principal calculated from Eq. (1) is no more than the fracture strength of BK7. Then, the size of the damage zone induced by lateral cracks could be determined.

In order to validate the prediction model proposed here, the predicted damage zone size induced by lateral cracking was compared with the experimental results as well as those based on Jing's model (see Fig. 9). The trends of the two prediction models are similar, that is, the predicted damage zone size monotonically increases with normal load. However, it is clear that, for a given normal load, the predicted damage zone size based on the present model is always greater than that based on Jing's model. As indicated by Eqs. (1), (3) and (9), the damage zone size is strongly influenced by the contact zone size of the indenter. In Jing's model, the recovery of the material after complete removal of the indenter was not considered, and the contact zone size was assumed as the half-width of the scratch groove. As a result, the damage zone size based on Jing's model was underestimated.

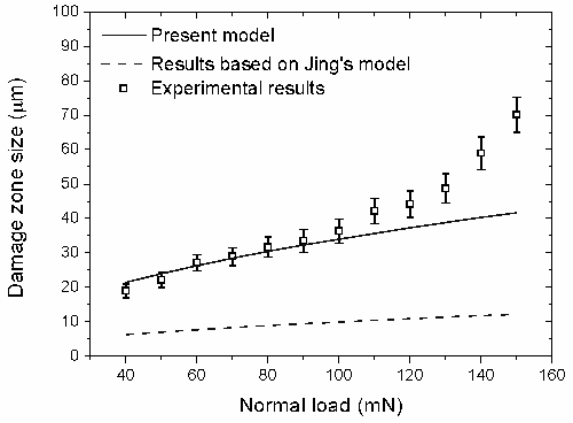

Fig. 9. Damage zone size induced by lateral cracking vs. applied normal load.

In general, the results of the present model are in reasonable agreement with those obtained from scratch experiments when normal load is from 0 to 100mN (corresponding scratch depth=0~0.9μm). It is worth noting that the scratch depth in the range from 0 to 0.9μm is comparable to the maximum grit depth in precision and ultra-precision grinding of brittle materials [24, 25]. Therefore, based on the parameters in precision and ultra-precision grinding, the present model might be useful for evaluating the intensity of the interaction between neighboring grits and estimating the material removal volume.

It is further noted that, under relatively high normal loads, the local stress concentration at the crack tip becomes significant, which makes lateral cracks easier to propagate and finally leads to greater damage zone size. In this study, however, the local stress concentration at the crack tip is not taken into consideration. Therefore, when normal load is higher than about 100mN, the damage zone size predicted from the present model is smaller than the experimental results.

4. Conclusions

Micron and sub-micron scale scratch tests were conducted on optical glass BK7 with Vickers indenters. Three types of surface cracking, namely lateral cracking, radial cracking and cracking in front of the moving indenter, were observed around the scratch groove. Before cracks appear in front of the moving indenter, there is a linear relationship between the normal load and the square of the scratch depth even when lateral cracks occur around the scratch groove. The square of the scratch depth increases with the normal load in an unstable manner when normal load is greater than 130mN.

Lateral cracking is considered to be the main cracking type due to its large damage size and low crack initiation load. The contact zone size of the indenter was estimated based on the measurements of the scratch and residual depths. The plastic zone size as well as the sliding blister field strength was expressed as a function of the contact zone size. A prediction model for the size of damage zone induced by lateral cracking

was developed and was compared with the experimental results. It was found that, under relatively small normal load (i.e., no more than 100mN), the predicted results were in general agreement with the experimental data. This prediction model might be helpful to gain insight into evaluating the intensity of the interaction between neighboring and estimating the material removal volume during precision and ultra-precision grinding. It should be noted that the model is suitable for brittle materials with the amorphous nature (e.g., optical glasses). For polycrystalline materials, such as structural ceramics, however, the effect of the grain should be taken into consideration.

When normal load is higher than about 100mN, the difference between the predicted and experimental results becomes large. Our future work is focused on the influence of the stress concentration at the crack tip on the propagation of lateral cracking and further predicting the damage zone size under relatively high normal loads.

Acknowledgment

The authors gratefully acknowledge the financial support provided by the Shanghai Science and Technology Development Foundation of China (grant No. 07111002). This work was partially supported by the Foundation for Innovative Research Groups of the National Natural Science Foundation of China (Grant No. 50821003). The authors are also grateful for the editors and reviewers who made constructive comments.

Nomenclature

A	:	Strength of indentation-induced blister field
a_r	:	Half-width of scratch groove
a_s	:	Contact area
B	:	Strength of the sliding blister filed
b	:	Depth of plastic deformation zone
$d\xi$	:	Increment of scratch length
E	:	Young's modulus
H	:	Vickers hardness
h_r	:	Residual depth
h_s	:	Scratch depth
L	:	Pileup zone size
l	:	Scratch length
P	:	Normal load
Q	:	Tangential load
W	:	Damage zone size
X	:	Rheological factor
ΔV_i	:	Increased volume in inelastic deformation zone during an indentation
ΔV_s	:	Increased volume in inelastic deformation zone during a scratch
θ	:	Semi-apical angle of the indenter
μ	:	Depth ratio
ν	:	Poisson's ratio
σ_f	:	Fracture strength
σ_y	:	Yield stress
σ_{yy}	:	Normal stress along y-direction
σ_{zz}	:	Normal stress along z-direction
τ_{yz}	:	Tangential stress

References

[1] A. B. van Groenou, N. Mann and J. B. D. Veldkamp, Single-point scratches as a basis for understanding grinding and lapping, *Science of Ceramic Machining and Surface Finishing,* 2 (1997) 43-60.

[2] G. Subhash and R. Bandyo, A new scratch resistance measure for structural ceramics, *J. Am. Ceram. Soc.,* 88 (2005) 918-925.

[3] G. Subhash and M. Klecka, Ductile to brittle transition depth during single-grit scratching on alumina ceramics, *J. Am. Ceram. Soc.,* 90 (2007) 3704-3707.

[4] M. Nakamura, T. Sumomogi and T. Endo, Evaluation of surface and subsurface cracks on nano-scale machined brittle materials by scanning force microscope and scanning laser microscope, *Surf. Coat. Technol.,* 169-170 (2003) 743-747.

[5] R. Thonggoom and P. D. Funkenbusch, Transition in material removal behavior during repeated scratching of optical glasses, *J. Mater. Sci.,* 40 (2005) 4279-4286.

[6] K. Li, Y. Shapiro and J. C. M. Li, Scratch test of soda-lime glass, *Acta Mater.,* 46 (1998) 5569-5578.

[7] O. Desa and S. Bahadur, Material removal and subsurface damage studies in dry and lubricated single-point scratch tests on alumina and silicon nitride, *Wear,* 225-229 (1999) 1264-1275.

[8] V. Le Houérou, J. C. Sangleboeuf, S. Dériano, T. Rouxel and G. Duisit, Surface damage of soda–lime–silica glasses: indentation scratch behavior, *J. Non-Cryst. Solids,* 316 (2003) 54-63.

[9] M. Klecka and G. Subhash, Grain size dependence of scratch-induced damage in alumina ceramics, *Wear,* 263 (2008) 137-148.

[10] E. H. Yoffe, Elastic stress fields caused by indenting brittle materials, *Philos. Mag.,* 46 (1982) 617-628.

[11] Y. Ahn, T. N. Farris and S. Chandrasekar, Sliding microindentation fracture of brittle materials: Role of elastic stress fields, *Mech. Mater.,* 29 (1998) 143-152.

[12] Y. Ahn, N. G. Cho, S. H. Lee and D. Lee, Lateral crack in abrasive wear of brittle materials, *JSME International Journal Series A,* 46 (2004) 140-144.

[13] X. N. Jing, S. Maiti and G. Subhash, A new analytical model for estimation of scratch-induced damage in brittle solids, *J. Am. Ceram. Soc.,* 90 (2007) 885-892.

[14] D. M. Marsh, Plastic flow in glass, *Proc. Roy. Soc. A,* 279 (1964) 420-435.

[15] V. H. Bulsara and S. Chandrasekar, Direct observation of contact damage around scratches in brittle solids, *Window and Dome Technologies and Materials V,* 3060 (1997) 76-88.

[16] H. P. Kirchner, Comparison of single-point and multipoint grinding damage in glass, *J. Am. Ceram. Soc.,* 67 (1984)

347-353.
[17] J. L. Bucaille, E. Felder and G. Hochstetter, Mechanical analysis of the scratch test on elastic and perfectly plastic materials with the three-dimensional finite element modeling, *Wear,* 249 (2001) 422-432.
[18] J. M. Antunes, L. F. Menezes and J. V. Fernandes, Three-dimensionl numerical simulation of Vickers indentation tests, *Int. J. Solids Struct.,* 43 (3-4) (2006) 784-806.
[19] C. Wei, H. He, Z. Deng, J. Shao and Z. Fan, Study of thermal behaviors inCO2 laser irradiated glass, *Opt. Eng.,* 44 (2005) 1-4.
[20] J. C. Lambropoulos, T. Fang, P. D. Funkenbusch, S. D. Jacobs, M. J. Cumbo and D. Golini, Surface microroughness of optical glasses under deterministic microgrinding, *Appl. Opt.,* 35 (22) (1996) 4448-4462.
[21] K. L. Johnson, *Contact Mechanics*, *Cambridge University Press*, Cambridge, UK (1985).
[22] C. Ramond-Angélélis, Analyse mécanique des essais d'indentation sur matériaux élasto-plastiques homogènes ou multi-couches. Application à la caractérisation de la rhéologie et de la tenue mécanique des films minces, Ph.D. thesis, *Ecole Nationale Supérieure des Mines de Paris* (1998).
[23] R. F. Cook and G. M. Pharr, Direct observation and analysis of indentation cracking in glass and ceramics, *J. Am. Ceram. Soc.,* 73 (1990) 787-817.
[24] J. E. Mayer and G. P. Fang, Effect of Grinding Parameters on Surface Finish of Ground Ceramics, *CIRP Annals,* 44 (1) (1995) 279-282.
[25] M. J. Chen, Q. L. Zhao, D. Li and S. Dong, The critical conditions of brittle-ductile transition and the factors influencing the surface quality of brittle materials in ultra-precision grinding, *J. Mater. Process. Technol.,* 168 (2005) 75-82.

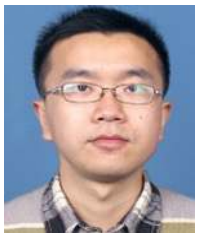

Weibin Gu received his B.S. degree in mechanical engineering from Nanjing University of Science and Technology, Nanjing, China. He is currently a graduate student of Master-Doctor combined program in Shanghai Jiao Tong University, Shanghai, China. His research interests include grinding mechanisms of hard-brittle materials and grinding process simulation.

Zhenqiang Yao received his B.S. and M.S degrees in mechanical engineering from Shanghai Jiao Tong University, Shanghai, China. He received his Ph.D. from the joint training program of University of Warwick (UK) and Shanghai Jiao Tong University (China) in 1993. He is currently a professor in mechanical engineering of Shanghai Jiao Tong University, China. His research interests include machining mechanisms of hard-brittle materials and machining process simulation.